MEMS-Based RF Channel Selection for True Software-Defined Cognitive Radio and Low-Power Sensor Communications

Clark T.-C. Nguyen, University of California at Berkeley

ABSTRACT

An evaluation of the potential for MEMS technologies to realize the RF front-end frequency gating spectrum analyzer function needed by true software-defined cognitive radios and ultra-low-power autonomous sensor network radios is presented. Here, RF channel selection, as opposed to band selection that removes all interferers, even those in band, and passes only the desired channel, is key to substantial potential increases in call volume with simultaneous reductions in power consumption. The relevant MEMS technologies most conducive to RF channel-selecting front-ends include vibrating micromechanical resonators that exhibit record on-chip *Q*s at gigahertz frequencies; resonant switches that provide extremely efficient switched-mode power gain for both transmit and receive paths; medium-scale integrated micromechanical circuits that implement on/off switchable filter-amplifier banks; and fabrication technologies that integrate MEMS together with foundry CMOS transistors in a fully monolithic low-capacitance single-chip process. The many issues that make realization of RF channel selection a truly challenging proposition include resonator drift stability, mechanical circuit complexity, repeatability and fabrication tolerances, and the need for resonators at gigahertz frequencies with simultaneous high Q (>30,000) and low impedance (e.g., 50 Ω for conventional systems). Some perspective on which resonator technologies might best achieve these simultaneous attributes is provided.

INTRODUCTION

Although somewhat poorly publicized, microelectromechanical systems (MEMS)-based devices already play important, in some cases critical, roles in wireless communication devices. Examples of MEMS devices already in wireless systems include piezoelectric film bulk acoustic resonators (FBARs) used for front-end duplexer filters in cell phones, high-Q capacitive-gap transduced resonators used in low-end timing oscillators that are also used in a myriad of applications beyond wireless [1], and more recently, tunable/switchable capacitors for front-end amplifier-to-antenna impedance matching [2] that help to lower transmit power consumption. But this list only scratches the surface of what is possible. Indeed, if newer MEMS-based devices on the horizon are successful, much bigger advances may soon be on hand that just might catalyze key communication architectural paradigm shifts needed to address fast-growing demands for advanced communication concepts like true software-defined cognitive radio and ultra-low-power radios for autonomous energy harvesting sensor networks.

In particular, recent advances in vibrating radio frequency (RF) MEMS technology that yield on-chip resonators with *Q*s over 40,000 at 3 GHz [3, 4] and excellent thermal [5] and aging stability [6] have now positioned vibrating micromechanical devices as strong candidates for inclusion in a number of future wireless communication subsystems, from cellular handsets to PDAs to low-power networked sensors [7]. As mentioned, early startups have already sprouted to take advantage of this technology for timekeeper applications [1]. Indeed, the timing of this technology seems well placed for wireless markets, whose requirement for multimode reconfigurability fuels a need for multiple high-Q resonators on a single chip to prevent the cost of discrete high-Q passives from obviating that of the integrated circuits [7].

But the benefits of vibrating RF MEMS technology go far beyond mere component replacement. In fact, the extent of the performance and economic benefits afforded by vibrating RF MEMS devices grows exponentially as researchers and designers begin to perceive them more as building blocks than as standalone devices. For example, when integrated into

0163-6804/13/$25.00 © 2013 IEEE

micromechanical circuits, in which vibrating mechanical links are connected into larger, more general networks, previously unachievable signal processing functions become possible, such as reconfigurable RF channel-selecting filter banks, ultra-stable reconfigurable oscillators, mechanical power converters, mechanical power amplifiers, frequency domain computers, and frequency translators. This article focuses on the MEMS technologies most suitable to micromechanically realizing the frequency gating RF front-end needed by true software-defined cognitive radios and ultra-low-power radios for autonomous sensor networks.

Software-Defined Cognitive Radio

The increasing desire for reconfigurable radios capable of adapting to any communication standard at any location across the world has spurred great interest in the concept of a software-defined radio (SDR) [8, 9], in which the frequencies and modulation schemes of any existing communication standard can be produced in real time by simply calling up an appropriate software sub-routine. Arguably, the ultimate rendition of such a radio would realize all radio functions, including the RF front-end, digitally, using a programmable microprocessor. To achieve this, the analog-to-digital converter (ADC) that normally resides near the baseband circuits of a conventional receiver would need to be placed as close to the antenna as possible so that as much signal processing as possible could be done digitally.

Ideally, in a true SDR implementation, all functions would be programmable, including any pre-filtering. In other words, a true SDR would not require any specific front-end hardware, i.e., no hardwired mode-specific switches or filters. This is where present-day technology is grossly lacking. To date, published attempts to achieve an SDR have required practical compromises, especially in the RF front-end, where designs in the most recent literature [10] continue to rely on very specific band-select filters that must be switched in and out as the communication mode changes. Interestingly, these designs often cite MEMS technology as a cost-reducing measure, whereby the size and cost of the many filters needed for SDR application (e.g., more than 20) is mitigated by an expectation that many MEMS-based filters can be fabricated onto a single chip, perhaps together with a multi-throw switch [7]. While probably true, this use of MEMS technology makes no advance against the need for hardwired mode-specific circuitry, so is quite conservative and falls well short of what is possible.

This begs the question: To what extent are front-end filters even necessary? Again, ideally the ADC would immediately follow the antenna(s) and would have an input bandwidth covering the full spectrum of received signals (e.g., 3 GHz). Alas, practically, a frequency gating function must precede the ADC to remove blockers (i.e., out-of-channel interferers) that can be many orders stronger than the desired signal at the receive antenna. Removing such blockers relaxes the ADC's dynamic range and power requirements, which otherwise would be too excessive for portable applications. For reasonable ADC power consumption, all blockers, even those very close to the desired channel and within its communication standard's band, must be removed.

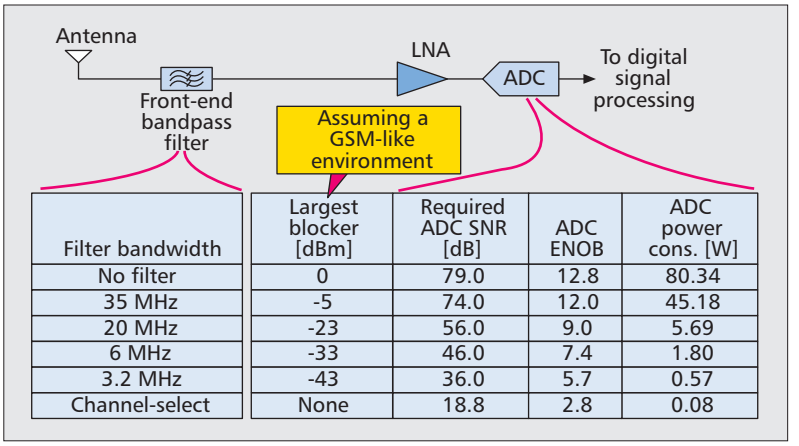

Filter bandwidth	Largest blocker [dBm]	Required ADC SNR [dB]	ADC ENOB	ADC power cons. [W]
No filter	0	79.0	12.8	80.34
35 MHz	-5	74.0	12.0	45.18
20 MHz	-23	56.0	9.0	5.69
6 MHz	-33	46.0	7.4	1.80
3.2 MHz	-43	36.0	5.7	0.57
Channel-select	None	18.8	2.8	0.08

Figure 1. *Dynamic range and consequent power consumption required by an ADC designed to accept a 3GHz-wide input RF spectrum for an SDR in a blocker environment identical to that assumed by the GSM standard.*

To more concretely convey the importance of filtering out interferers before they reach the ADC input, Fig. 1 summarizes the signal-to-noise ratio (SNR) and consequent needed power consumption required by a wide open (i.e., 3 GHz) bandwidth, state-of-the-art ADC used in a true SDR assuming various prefiltering bandwidths to remove interferers. Here, a 3 GHz bandwidth ADC is considered in this example, mainly in the interest of exploring the most ideal case of an SDR capable of receiving several transmissions at once anywhere in its 3 GHz bandwidth. To keep things simple, this analysis assumes a GSM-like blocking scenario with an input noise requirement of –120.8 dBm in a 200 kHz bandwidth [11], which rises to –79 dBm when adjusted for input to a wider (3 GHz) bandwidth ADC. As shown, with no front-end filtering, the 0 dBm out-of-band blockers assumed in the GSM standard [11] demand an ADC SNR of 79 dB. To attain this SNR, the ADC would need an equivalent number of bits (ENOB) of 12.8, which in recent transistor technology with an ADC *FOM* of 1.83 pJ/bit [12] would consume more than 80 W of power!

As the bandwidth of prefiltering decreases, more interferers are suppressed, and the needed SNR of the ADC relaxes. Note, however, from Fig. 1 that even the 35 MHz bandwidth of a conventional preselect filter (used in cell phones today) is still grossly insufficient for SDR, as the interferers that remain after its filtering force the 3 GHz bandwidth ADC to consume a still highly impractical 45 W. Indeed, as shown in Fig. 1, reasonable ADC power consumption on the order of 80 mW is not achieved until the filter bandwidth corresponds to that needed to eliminate all interferers (i.e., to select the desired channel and only this channel). For GSM, where emissions are regulated so that each 200 kHz

channel is sandwiched by empty spectrum in any given cell, this would require a filter bandwidth of 600 kHz, or a percent bandwidth at 1.8 GHz on the order of 0.03 percent — two orders of magnitude smaller than the 3 percent of conventional preselect filters!

It follows that to eliminate all interferers and pass only the desired signal, a programmable frequency gating device or circuit is needed that can pass and reject tiny (e.g., 0.03 percent bandwidth) RF frequency channels at will along the entire 3 GHz input frequency span. The need for such a small percent bandwidth makes this especially difficult, since the smaller the percent bandwidth, the higher the needed Qs of the resonators comprising a given filter to maintain reasonable insertion loss. For example, the constituent resonators making up a 3 GHz, 0.03 percent (1 MHz) bandwidth, 0.01 dB ripple, 4-resonator Chebyshev filter would require Qs > 30,000 just to maintain an insertion loss below 3 dB [13]. To further complicate things, it is often the case that the higher the Q of a resonator, the less tunable it is. In fact, at the time of this writing, there are no existing on-chip resonator technologies capable of achieving Qs > 30,000 while also being continuously tunable over a 3 GHz span.

Fortunately, MEMS technology offers an alternative method of achieving the desired programmable frequency gate that dispenses with the need to tune a given resonator's frequency over a wide range. In particular, being a wafer-level manufacturing technology similar to those used for integrated transistor circuits, MEMS encourages designers to use mechanical devices the same way transistors are used: in massive numbers. So instead of restricting the implementation of a programmable frequency gate to a single tunable filter, MEMS technology allows realization of the same programmable frequency gate via a bank of on/off switchable micromechanical filters, as depicted in Fig. 2a, where each filter is realized using an interconnected network of micromechanical resonators (to be described).

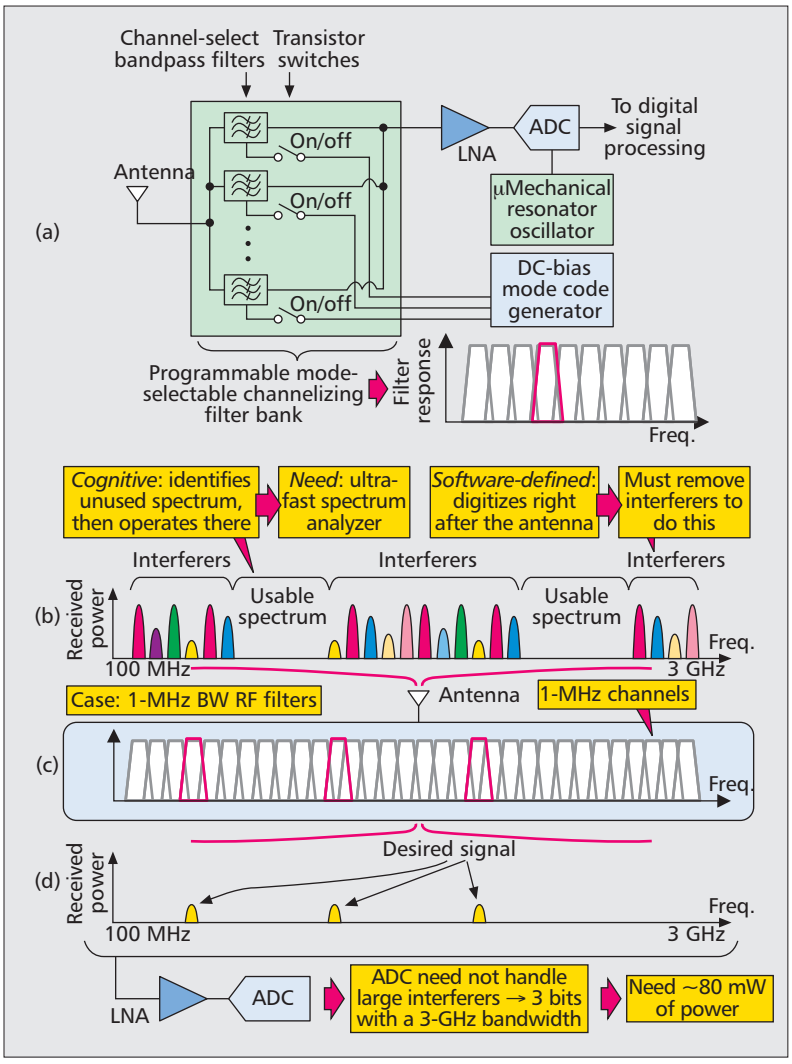

Figure 2. *a) System block diagram for an SDR front-end utilizing a micromechanical RF channel-select filter network to realize a frequency gating function. When one (or more) filters are turned "on," with all others "off," the filter bank realizes a frequency gate. When all filters are turned "on," the bank realizes a real-time spectrum analyzer that could be used to assess the entire received spectrum and determine what frequencies might be permissible to operate a cognitive radio; b) cartoon of the typical power spectrum that might be received by an antenna-terminated spectrum analyzer atop a tall building at a given moment in time. Here, many channels are unused at this instant, and thus are available for use by a cognitive radio; c) on/off configuration of filters in the RF channelizing filter bank of a) that selects specific channels to pass and reject; d) output of the filter bank directed to the ADC containing only desired channel signals and no blockers, allowing substantially lower ADC power consumption, per Fig. 1.*

Cognitive Radio

The programmable frequency gate of Fig. 2a is not only applicable to SDR, but also to cognitive radio. In particular, beyond SDR, many researchers are further exploring the possibility of a cognitive radio that is not restricted to operation only in a prescribed frequency band (which is the situation today), but that can seek out unused spectrum and operate there until a higher-priority user shows up, in which case the radio must move to another unused frequency. Such a scheme recognizes that although the entirety of available spectrum has already been allocated to someone (or some purpose) by a regulating body, such as the Federal Communications Commission (FCC) in the United States, the prescribed users do not always use their spectrum. In particular, the actual used spectrum at any given moment in time might look as shown in Fig. 2b, which plots a cartoon of the typical power spectrum that might be received by a (wideband) antenna-terminated spectrum analyzer atop a tall building at a given moment in time. Here, some bands are in use at the instant the spectrum is taken, but many other bands are unused. As mentioned, a cognitive radio would seek to operate in any one of the empty bands (or channels) labeled "usable spectrum." However, in order to determine which bands are empty, such a radio would need to first be able to take a snapshot of the power spectrum. This would require a spectrum analyzer and a very fast one at that, since the cognitive radio would need to check spectrum usage every few milliseconds in order to know when to vacate a channel when a higher-priority user begins to use it. Thus, the needed spectrum analyzer must both be extremely fast and consume very little power in portable handheld applications.

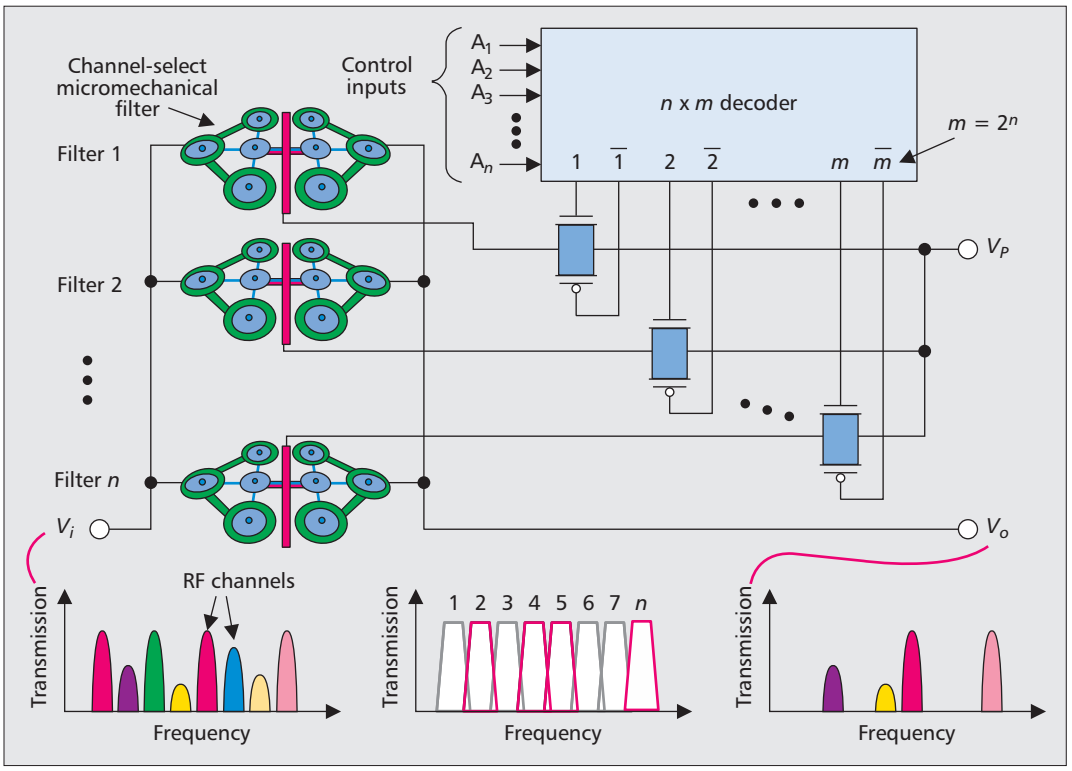

Figure 3. *Schematic of an RF channel-select micromechanical filter bank, with an example showing how various input frequencies can be simultaneously selected via mere application or removal of resonator dc-biases. In the bottom plots, filters 2, 4, 5, and* n *are on, while all others are off.*

Instead of restricting the implementation of a programmable frequency gate to a single tunable filter, MEMS technology allows realization of the same programmable frequency gate via a bank of on/off switchable micro-mechanical filters, where each filter is realized using an interconnected network of micromechanical resonators.

Unfortunately, presently available methods for spectrum analysis cannot achieve both speed and lower power simultaneously. In particular, fast spectrum analyzers based on fast Fourier transform (FFT) circuits would require excessive power to cover a 3 GHz band; and lower-power swept filter spectrum analyzers cannot sweep their filters faster than a time proportional to the filter settling time, and hence are not fast enough. On the other hand, MEMS technology seems very well suited to this problem. In particular, the very mechanical circuit of Figs. 2a and 2c that implements a frequency gate also functions as a spectrum analyzer when all of its filters are turned on simultaneously. The resulting spectrum analyzer is both extremely fast, since little or no filter sweeping would be needed, and very low in power consumption, since it is virtually all passive. As a result, the micromechanical circuit of Fig. 2a realizes both the frequency gating shown in Figs. 2c and 2d needed for SDR and the fast, low-power spectrum analyzer needed for cognitive radio, and hence effectively realizes what might be called a frequency gating spectrum analyzer well tailored for software-defined cognitive radio.

Of course, such a mechanical circuit is only useful if simultaneous high-Q and low impedance can be obtained, if switching of filters can be done quickly and without additional insertion loss, and if MEMS fabrication technology can support a very large-scale integrated (VLSI) mechanical circuit. Examples of MEMS technologies that might address these issues and make possible the described frequency gating spectrum analyzer are now presented.

Micromechanical Programmable Frequency Gating Spectrum Analyzer

Figure 3 presents a more detailed schematic showing one approach to implementing the frequency gating spectrum analyzer of Fig. 2, using as building blocks capacitive-gap transduced micromechanical disk resonators, summarized in Fig. 4. Among other information, Figs. 4d and 4e present the scanning electron micrograph (SEM) and measured frequency characteristic for one such resonator: a 1.51 GHz radial-contour mode disk resonator that achieves an impressive on-chip room temperature Q of 11,555 in vacuum, and 10,100 in air [4]. This device consists of a 20-μm-diameter 3-μm-thick polydiamond disk suspended by a polysilicon stem self-aligned to be exactly at its center, all enclosed by doped polysilicon electrodes spaced less than 80 nm from the disk perimeter. It can be excited into resonance via a combination of dc and ac voltages that can be chosen to turn the device "on" or "off" [14], very conveniently realizing the switchability required by the circuits of Figs. 2 and 3. When vibrating in its radial contour mode, the disk expands and contracts around its perimeter, in a motion reminiscent of breathing, and in what effectively amounts to a high-stiffness high-energy extensional mode. Since the center of the disk corresponds to a node location for the radial contour vibration mode shape, anchor losses through the supporting stem are greatly suppressed, allowing this design to retain a very high Q even at this UHF

The latest advancement in MEMS resonator technology that recently made available resonant mechanical switches (dubbed "resoswitches") offers a method for realizing amplification without the need for transistors and their associated quiescent current draws.

frequency. A version of this device at 498 MHz achieves a Q of 55,300 in vacuum [4], which is more than enough to implement the needed tiny percent bandwidth filters for the described RF frequency gating spectrum analyzer. More recent devices based on ring geometries have now achieved Qs > 40,000 at 3 GHz [3], so as far as Q is concerned, MEMS technology seems to fit the bill.

Recognizing this, Fig. 4f presents a mechanical circuit fabricated via the process of [15] that realizes a switchable bank of side-by-side mechanical filter passbands, each selectable by dc-bias voltages applied to the resonators that form them. As shown, this mechanical circuit comprises several identical resonator elements coupled by mechanical links of various designed lengths attached at very specific locations on the

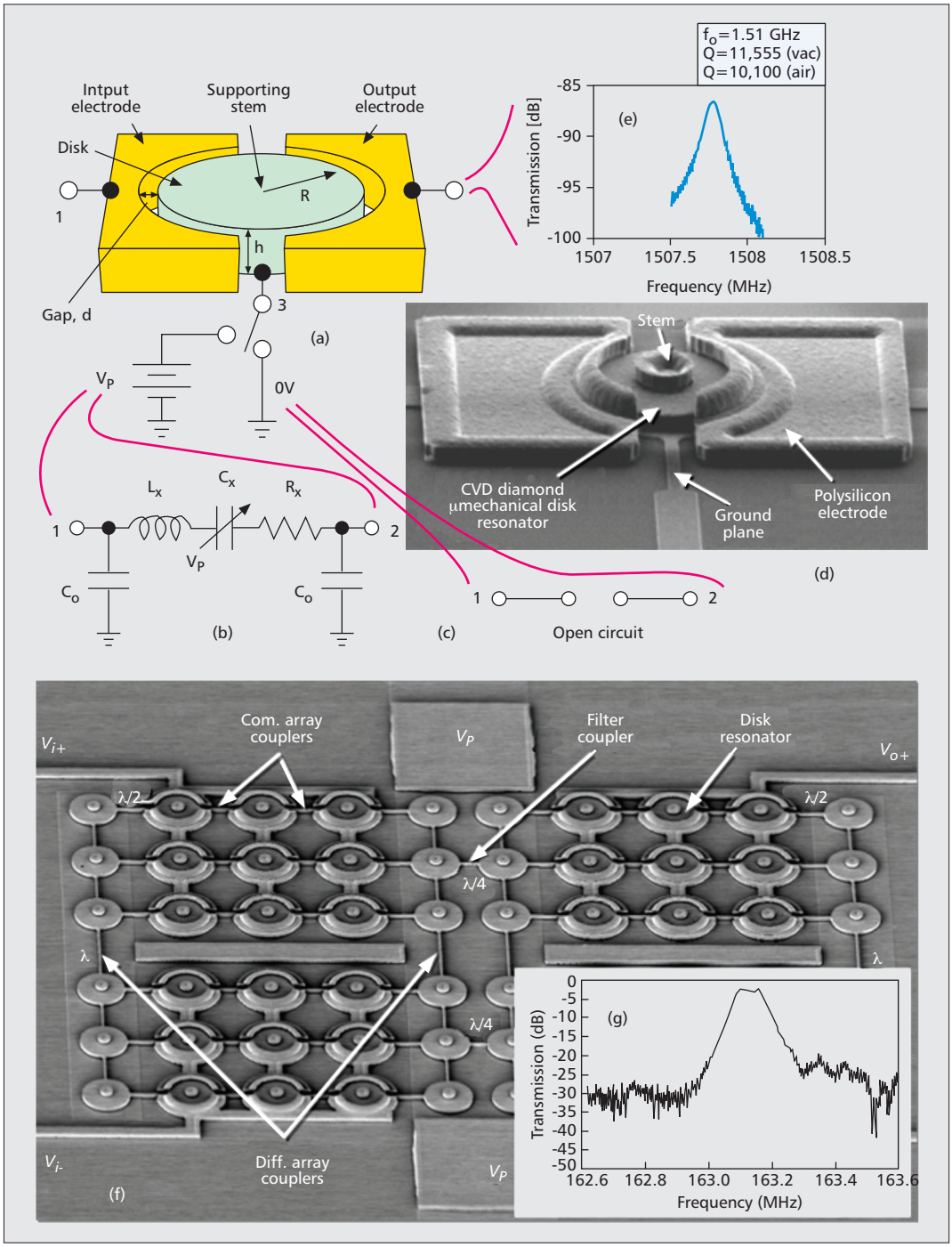

Figure 4. *Summary of the capacitive-gap transduced micromechanical disk resonator and its use in a mechanical filter circuit: a) perspective-view illustration, indicating input port 1, which receives the input sinusoidal voltage, output port 2, from which the output motional current is sensed, and bias port 3, which determines whether the device is b) "on" when a dc-bias is applied, in which case it behaves as an LCR tank, or c) "off" when the port is grounded; d) SEM of a 1.51 GHz μmechanical radial mode disk resonator; e) measured frequency response; f) μmechanical circuit using multiple coupled disk resonators to achieve the bandpass filter response of (g).*

resonators. Briefly, the center frequency of each switchable passband is determined primarily by thevkg@bell-labs.comvkg@bell-labs.com (identical) frequencies of the constituent resonators vibrating in the mode corresponding to the selected passband, while the bandwidths of the passbands and the spacings between them are determined largely by ratios of the stiffnesses of the various coupling beams to those of the resonators they couple at the attachment locations. Figure 4g presents a measurement of the lowest frequency switched-mode passband, which has a 0.06 percent bandwidth with a 2.43 dB insertion loss.

The complete structure of Fig. 4f comprises a medium-scale integrated (MSI) mechanical circuit that can be equated to an equivalent electrical circuit [15], with a one-to-one correspondence between mechanical and electrical elements. The values of the circuit elements are specified by the lateral dimensions of the associated mechanical elements, so the whole structure is amenable to automatic generation by a computer-aided design (CAD) program. Such a program could also automatically generate the layout required to achieve a specific filter specification, making the realization of a VLSI circuit of such filters ideally as convenient as for VLSI transistor integrated circuits (ICs).

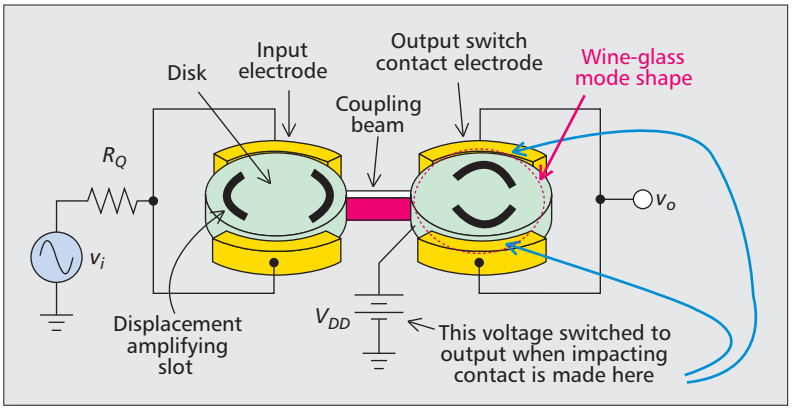

Figure 5. *Perspective illustration of a resoswitch filter-amplifier under an appropriate bias and excitation configuration. Here, the mechanically coupled disks are designed to operate in wine-glass modes, and slots are used to affect displacement amplification, where displacement is larger along a slot axis since the stiffness along this axis is smaller than that along the orthogonal axis. This displacement amplification ensures that impacting does not occur along the input axis when it occurs along the output switch axis, where it periodically connects the output to* V_{DD}*, sending its power to the output node, and thus serving as a power amplifier. The whole structure provides both channel-select filtering and power amplification.*

Ultra-Low-Power Radios for Sensor Networks

Indeed, if achievable, switchable banks of front-end filters with very small channel-selecting bandwidths would be just as beneficial for ultra-low-power receivers (e.g., needed for sensor networks) as for the described SDR. As detailed in [16], with all blockers removed, the oscillator phase noise and dynamic ranges of the LNA and mixer in any RF front-end could be relaxed enormously, to the point where highly nonlinear (and thus low-power) designs of these functions might be used. For example, one desirable design might dispense entirely with LNA linearity and just allow the amplifier to rail out, amplifying a tiny sinusoidal frequency shift keyed (FSK) input signal to a large square wave FSK signal easily processed by a discriminator, and all with minimal concern for intermodulation or other forms of blocker-generated spurious signals. Merely reducing the quiescent drain current of a conventional LNA should accomplish this. Unfortunately, the degree to which drain current can be reduced is still constrained by noise considerations.

Interestingly, the latest advancement in MEMS resonator technology, which recently made resonant mechanical switches (dubbed "resoswitches") available [17], offers a method for realizing amplification without the need for transistors and their associated quiescent current draws. As described in Fig. 5, the resoswitch is similar to a conventional micromechanical resonator, but differs in that it provides displacement gain made possible by both high Q at resonance and structural design (e.g., stiffness engineering using slots and a coupling beam), and its output resonator is designed to actually impact an output electrode during vibration. If the resonator and electrode are constructed in conductive materials, this impacting effectively closes a low-loss switch with a very large "off" to "on" transition slope, many times steeper than offered by any semiconductor switch. This means a power supply connected to the output resonator structure, as shown in Fig. 5, can be switched directly to a filter's output electrode at an input FSK frequency, just as occurs in any transistor switch-based gain circuit, but in this case, without quiescent current draw when there is no input signal and with a preceding channel-selecting filter function that removes blockers to allow this degree of amplifier nonlinearity.

The resoswitch device is equally useful when employed on the transmit side. In particular, similar to traditional (non-resonant) RF MEMS switches, the switch figure of merit (FOM_{sw}) for a resoswitch device is on the order of 60 THz, which is two orders of magnitude higher than the 600 GHz typical of transistor switches. This should translate to substantially better drain efficiency when a switched-mode (Class E) power amplifier employs a resoswitch device instead of presently used semiconductor switches. Predicted efficiencies are higher than 90 percent, to be compared with the 65 percent attained using gallium arsenide (GaAs) transistor switches [18].

This savings in transmit power is essential for sensor networks, for which transmit power can be as or more important than receive power when sleep strategies are utilized to minimize receive power. Ultimately, both receive and transmit power savings described in the above example would constitute welcome and extremely important savings that can help to enable the massive "set and forget" wireless sensor networks foreseen by many.

It should be noted that the above is only one of many ultra-low-power receiver concepts possible if RF channel selection (as opposed to band selection) were truly available. For example, as

Similar to traditional (non-resonant) RF MEMS switches, the switch figure of merit (FOM_{sw}) for a resoswitch device is on the order of 60THz, which is two orders of magnitude higher than the 600GHz typical of transistor switches.

explored in [19], super-regenerative receivers could also benefit substantially from channel-selecting RF front-ends. Other system-level energy savings can also be obtained by merely taking advantage of other high Q benefits, such as better timing stability, which would then allow longer sleep periods for sensors, where wake-up intervals are generally constrained by timing synchronization.

Practical Issues

Of course, anything that seems too perfect generally is not perfect, and the frequency-gating spectrum analyzer of Fig. 3 is no exception. Needless to say, there are practical problems that must be overcome, from impedance matching to frequency repeatability to frequency stability (e.g., against environmental variations), to integration with control electronics.

Impedance Matching

Unfortunately, although the Qs of the described resonators are exceptional, they are not easy to access, because the impedances they present are often much larger than that of the system using them. For example, many of today's board-level systems are designed around 50 Ω impedance, which is much smaller than the 2.8 kΩ termination resistors required by the 163-MHz differential disk array filter of [15]. Thus, even though this filter attains an impressively low insertion loss for a 0.06 percent bandwidth, it requires an L-network to match to 50 Ω.

One possible solution to this impedance problem is to use piezoelectric micromechanical resonators, such as the AlN ones of [20], which achieve single resonator impedances below 80 Ω. Unfortunately, the Qs are below 2900. Wafer-bonded thin quartz resonators have achieved Qs of 14,756 at 545 MHz and 7544 at 2.72 GHz [21], but these are still far short of the 30,000 needed for channel selection at RF. With further research, it is not unreasonable to expect that the Qs of thin-film piezoelectric resonators should eventually increase. Indeed, approaches to raising piezoelectric resonator Q are beginning to bear fruit, notably strategies that eliminate the Q-constraining effect of metal electrodes [22].

Still, capacitive resonator Qs are already sufficient for RF channel selection, and as mentioned, they do offer the equally important ability to self-switch, without any need for lossy external switches. So the question is, which is easiest to do: raise the Q of piezoelectric resonators, or reduce the impedance of capacitive resonators?

Recently published work asserts that the latter might be easier and is in fact happening as we speak. Indeed, several approaches are available that lower the motional resistance R_x of a capacitive resonator, all identifiable by simply studying its approximate expression:

$$R_x = \frac{\omega_o m_r}{Q} \cdot \frac{1}{V_P^2} \cdot \frac{d_o^4}{(\varepsilon A_o)^2} \quad (1)$$

where ω_o and m_r are the radian resonance frequency and equivalent mass, respectively, of the resonator; A_o and d_o are the electrode-to-resonator overlap area and gap spacing, respectively; V_P is the dc-bias applied to the resonator's conductive structure, shown in Fig. 4; ε is the permittivity in the electrode-to-resonator gap; and the geometric and voltage parameters are identified in Fig. 4. From Eq. 1, the value of R_x can be lowered by raising the dc-bias voltage V_P; increasing the electrode-to-resonator overlap area A_o [15]; increasing the electrode-to-resonator gap dielectric constant ε [23, 24]; and reducing the electrode-to-resonator gap d_o [25]. Clearly, by virtue of its fourth power dependence, the last of these is most effective. This is true not just for reducing motional resistance, but also, more important, for maximizing the mechanical filter figure of merit FOM_{mf}, given by

$$FOM_{mf} = \frac{1}{R_Q C_o} \cdot \frac{q}{m_r B} \cdot \frac{\varepsilon A_o}{d_o^3} \quad (2)$$

where R_Q is the needed filter termination resistance, C_o is the input overlap and shunt capacitance, q is a constant specific to the filter design (e.g., Chebyshev, Butterworth, 4-resonator) obtainable from a filter cookbook, and B is the filter bandwidth. The FOM_{mf} is related to the quantity (C_x/C_o) and is more useful than R_x for gauging efficacy in an actual RF filter, since it accounts for the interaction between motional resistance and input shunt capacitance C_o. From Eq. 2, decreasing gap spacing increases the FOM_{mf} much faster than other impedance-reducing approaches.

Also, contrary to popular belief, reducing gap spacing does not impact linearity as adversely as some may think. This can easily be seen from the experimentally verified expression for the third-order intermodulation input intercept point IIP_3 from [26]. For a 3-μm-thick 1 GHz radial-contour mode polysilicon disk resonator with a radius of 2.64 μm, dc-bias V_P of 10 V, and Q = 50,000, the IIP_3 expression from [26] predicts that simply changing gap spacing from 80 nm to 30 nm actually increases, not decreases, the IIP_3 from 25.1 dBm to 28.0 dBm, respectively! The reason for this is that although a reduction in gap spacing does indeed reduce the permissible amplitude of vibration, it also substantially reduces the R_x, so the amplitude of vibration needed to support a given power level is also much smaller.

At gigahertz frequencies, however, merely reducing the gap spacing is generally not sufficient if 50 Ω is desired. Indeed, Eq. 1 shows that R_x increases linearly with frequency. To circumvent this, one need only use a mechanical circuit, such as an array. Indeed, at 1 GHz, 50 Ω can be achieved using a mechanically coupled array of 24 3-μm-thick 2.64-μm-radius 50,000-Q polysilicon disks, each with V_P = 10 V and 30-nm electrode-to-resonator gap spacings, all occupying a total die area of only 45 × 29 μm^2 and possessing a substantially better IIP_3 than that of a single disk.

Whether via use of smaller gaps or alternative (piezoelectric) materials, recent research suggests that impedance-Q limitations of MEMS resonator technology will likely be overcome in

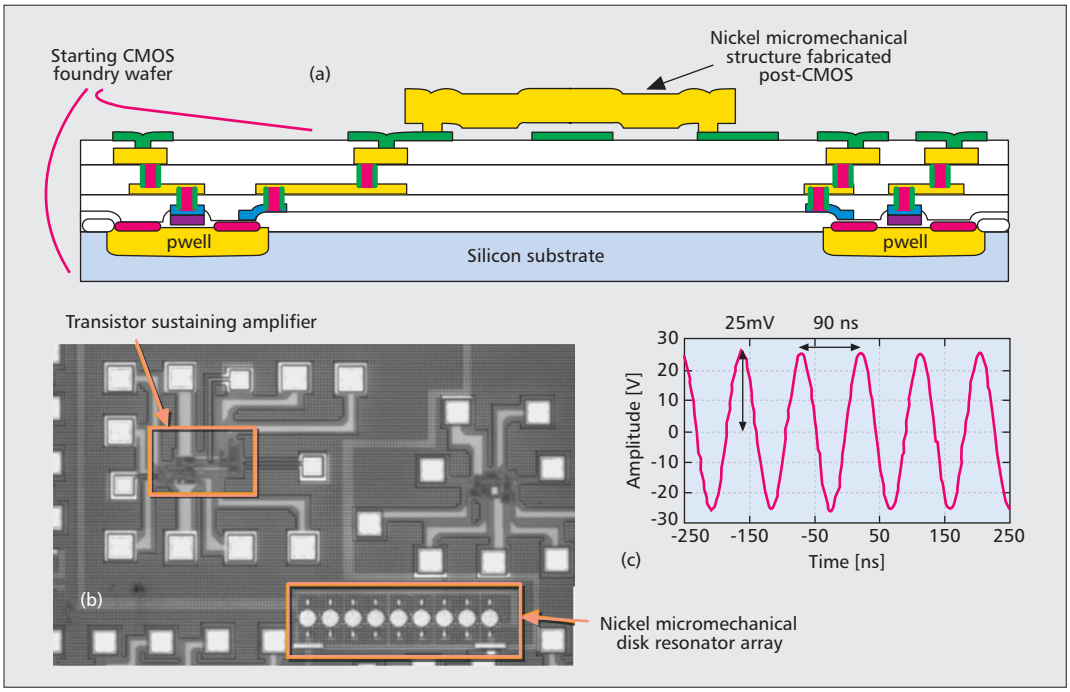

Figure 6. *a) Cross-section of the nickel MEMS-transistor integration process of [30]; b) die photo of a fully monolithic micromechanical resonator oscillator using this process; c) oscilloscope waveform.*

If voltage-controlled frequency tuning is to be employed, then some method for combining the massive numbers of MEMS devices with the needed electronic control devices (also in massive numbers) is needed. In most cases, this will demand wafer-level low-capacitance integration directly with transistors.

the near future. Ultimately, repeatability and control of frequencies on a massive scale will likely be the most difficult roadblocks to surmount.

Repeatability

Exhaustive measurements indicate that in a university fabrication facility, disk resonators such as that of Fig. 4 can be fabricated with frequency standard deviations on the order of 316 ppm and absolute tolerances on the order of 756 ppm [27]. Although this standard deviation is sufficient to realize 0.5 percent bandwidth filters without the need for any trimming, it is not sufficient for the 0.03 percent bandwidth filters needed for RF channel selection. Arraying of devices has been proven to reduce frequency standard deviation by a factor equal to the square root of the number of devices in the array [27], and this offers the option of using multiple spring-coupled resonators to replace each single resonator to achieve the degree of resonator matching needed to achieve 0.03 percent bandwidth filters without the need for trimming. As mentioned, for capacitive-gap transduced resonators, this sort of arraying is also beneficial if lower impedance is desired.

Ultimately, though, capacitive-gap MEMS resonators offer a much more potent defense against repeatability limitations: Their frequencies are voltage tunable via electrical stiffness, such as described in [5]. This means they need not be fabricated with exact frequency, but rather can be tuned to the right frequency. The tuning range is not large, on the order of only 0.01 percent/V at 500MHz and decreasing as frequency increases. Although small, the tuning range is certainly sufficient to fix filter response deficiencies, e.g., to achieve flat passbands or exactly a desired amount of group delay, or to move a filter response from one channel position in a bank to the adjacent one. This is all that's needed in the filter bank approach of Fig. 2.

If voltage-controlled frequency tuning is to be employed, then some method for combining the massive numbers of MEMS devices with the needed electronic control devices (also in massive numbers) is needed. In most cases, this will demand wafer-level low-capacitance integration directly with transistors.

MEMS-Transistor Integration

Integration is likely a must for the circuit of Fig. 2a, which does not explicitly show the transistor circuits needed to route the bias voltages that select (i.e., turn "on") the desired passbands. Given the complexity and density of the MEMS-to-transistor interconnections needed, it would be best if the MEMS and transistors were integrated together onto a single chip. Among approaches to doing this, MEMS-last ones are among the most attractive, since they allow the use of virtually any foundry for transistor circuits, which in turn minimizes cost.

To date, however, MEMS-last integration approaches have had little traction in consumer markets, partly because they require that processing temperatures for the MEMS stay below a ceiling that insures minimal degradation in transistor performance. Very few of the popular high-Q materials used for MEMS resonators, including the polydiamond and polysilicon materials of Fig. 4, are doable at temperatures under the needed ceiling, which may soon be around 300–400°C to accommodate the advanced low-k interconnect dielectrics targeted for future complementary metal oxide semiconductor (CMOS) generations [28]. Recent work, however, has

But before getting too excited about the possibilities, it is prudent to remind ourselves that much work still remains to control drift, manage complexity and repeatability for VLSI mechanical circuits, and lower the cost of MEMS-transistor integration.

shown (to the surprise of many) that metal materials can achieve high Q at high frequencies as long as the right resonator designs (e.g., disk geometries) are utilized [29]. Specifically, wineglass disk resonators with Qs > 20,000 have now been demonstrated in nickel material electroplated at only 50˚C. Capitalizing on this discovery, Fig. 6 presents the cross-section, die photo, and oscilloscope output waveform for a fully monolithic single-chip micromechanical resonator oscillator that combines nickel MEMS over foundry CMOS, recently demonstrated with reasonable high-Q oscillator performance [30]. With this, it may not be too long before top-level CMOS metals are used to implement micromechanical circuits, such as that of Fig. 6, allowing the whole system of Fig. 2 to reside on a single tiny silicon chip.

Conclusions

RF channel selection enabled by extremely high Qs > 30,000 and massive numbers of MEMS-based resonators stands to be a key enabler for not only software-defined cognitive radio, but also ultra-low-power radios for long-lived sensor networks. While these are already groundbreaking possibilities, perhaps the most compelling and important contribution of this technology is its propensity to encourage wireless designers to break existing assumptions (e.g., that the number of front-end high-Q passives must be minimized) and open their minds to the possibility of having Qs > 40,000 in abundance, allowing them to use as many high-Q passives as they please. Once this happens, an explosion of not only communication architectures, but even wireless standards, might ensue, and in turn foster proportional advancements in the capability of our wireless networks.

But before getting too excited about the possibilities, it is prudent to remind ourselves that much work still remains to control drift, manage complexity and repeatability for VLSI mechanical circuits, and lower the cost of MEMS-transistor integration. Needless to say, vibrant research efforts are already underway to address these issues. Perhaps communication hardware and standards designers alike should start considering RF channel selection for their forecasting roadmaps.

Acknowledgment

Much of the work summarized was supported by funding from the Defense Advanced Research Projects Agency (DARPA).

References

[1] W.-T. Hsu, "Recent Progress in Silicon MEMS Oscillators," *Proc. 2008 40th Annual Precise Tme and Time Interval Systems and Applications Meeting*, Reston, VA, Dec. 1–4, 2008.
[2] J. L. Hilbert, "RF-MEMS for Wireless Communications," *IEEE Commun. Mag.*, Aug. 2008, pp. 68–74.
[3] T. L. Naing *et al.*, "2.97-GHz CVD Diamond Ring Resonator with Q>40,000," *Proc. IEEE Int'l. Frequency Control Symp.*, Baltimore, MD, May 21–24, 2012.
[4] J. Wang *et al.*, "1.51-GHz Polydiamond Micromechanical Disk Resonator with Impedance-Mismatched Isolating Support," *Proc. 17th IEEE Int'l. Micro Electro Mechanical Systems Conf.*, Maastricht, The Netherlands, Jan. 25–29, 2004, pp. 641–44.
[5] W.-T. Hsu and C. T.-C. Nguyen, "Stiffness-Compensated Temperature-Insensitive Micromechanical Resonators," *Tech. Digest, 2002 IEEE Int'l. Micro Electro Mechanical Systems Conf.*, Las Vegas, NV, Jan. 20–24, 2002, pp. 731–34.
[6] B. Kim *et al.*, "Frequency Stability of Wafer-Scale Encapsulated MEMS Resonators," *Dig. of Tech. Papers, Transducers '05*, Seoul, Korea, June 2005, pp. 1965–68.
[7] C. T.-C. Nguyen, "MEMS Technology for Timing and Frequency Control," *IEEE Trans. Ultrason. Ferroelect. Freq. Contr.*, vol. 54, no. 2, 2007, pp. 251–70.
[8] J. Mitola, "The Software Radio Architecture," *IEEE Commun. Mag.*, May 1995, pp. 26–38.
[9] M. Dillinger, K. Madani, and N. Alonistioti, *Software Defined Radio: Architectures, Systems and Functions*, Wiley, 2003.
[10] V. Giannini *et al.*, "A 2-mm 0.1–5 GHz Software-Defined Radio Receiver in 45-nm Digital CMOS," *IEEE J. Solid-State Circuits*, vol. 44, no. 12, Dec. 2009, pp. 3486–98.
[11] J. C. Rudell *et al.*, "An Integrated GSM/DECT Receiver: Design Specifications," UCB Electronics Research Laboratory Memorandum, Memo#: UCB/ERL M97/82, Berkeley, CA, 1998.
[12] Texas Instruments ADC12D1800 Data Sheet.
[13] C. T.-C. Nguyen, "Integrated Micromechanical RF Circuits for Software-Defined Cognitive Radio," *Proc. 26th Symp. Sensors, Micromachines & Applied Systems*, Tokyo, Japan, Oct. 15–16, 2009, pp. 1–5.
[14] S.-S. Li *et al.*, "Self-Switching Vibrating Micromechanical Filter Bank," *Proc. Joint IEEE Int'l. Frequency Control/Precision Time & Time Interval Symp.*, Vancouver, Canada, Aug. 29–31, 2005, pp. 135–41.
[15] S.-S. Li *et al.*, "An MSI Micromechanical Differential Disk-Array Filter," *Dig. of Tech. Papers of the 14th Int'l. Conf. Solid-State Sensors & Actuators (Transducers'07)*, Lyon, France, June 11-14, 2007, pp. 307–11.
[16] C. T.-C. Nguyen, "Frequency-Selective MEMS for Miniaturized Low-Power Communication Devices," *IEEE Trans. Microwave Theory Tech.*, vol. 47, no. 8, Aug. 1999, pp. 1486–503.
[17] Y. Lin *et al.*, "Metal Micromechanical Resonant Switch for On-Chip Power Applications," *Tech. Digest, IEEE Int'l. Electron Devices Mtg.*, Washington, DC, Dec. 5–7, 2011.
[18] C. Meliani *et al.*, "A 2.4-GHz GaAs-HBT Class E MMIC Amplifier with 65 percent PAE," *Proc. IEEE MTT-S Int. Microwave Symp.*, Honollulu, Hawaii, 2007 June 3–8, 2007, pp.1087-1090.
[19] B. Otis, Y. H. Chee, and J. Rabaey, "A 400 uW-RX, 1.6mW-TX Super-Regenerative Transceiver for Wireless Sensor Networks," *Dig. Technical Papers, 2005 IEEE Int'l. Solid-State Circuits Conf.*, San Francisco, CA, 2005, pp. 396–606.
[20] G. Piazza, P. J. Stephanou, and A. P. Pisano, "Piezoelectric Aluminum Nitride Vibrating Contour-Mode MEMS Resonators," *J. Microelectromech. Sys.*, vol. 15, no. 6, Dec. 2006, pp. 1406–18.
[21] F. Stratton *et al.*, "A MEMS-based Quartz Resonator Technology for GHz Applications," *Proc. IEEE Int'l. Ultrasonics, Ferroelectrics, and Frequency Control 50th Anniv. Joint Conf.*, Montreal, Canada, Aug. 23–27, 2004, pp. 27–34.
[22] L.-W. Hung and C. T.-C. Nguyen, "Capacitive-Piezoelectric AlN resonators with Q > 12,000," Tech. Digest, *24th IEEE Int'l. Conf. Micro Electro Mechanical Systems*, Cancun, Mexico, Jan. 24–28, 2011.
[23] Y.-W. Lin *et al.*, "Vibrating Micromechanical Resonators with Solid Dielectric Capacitive-Transducer 'Gaps'," *Proc. Joint IEEE Int. Frequency Control/Precision Time & Time Interval Symp.*, Vancouver, Canada, Aug. 29–31, 2005, pp. 128–34.
[24] D. Weinstein and S. Bhave, "Internal Dielectric Transduction in Bulk-Mode Resonators," *J. Microelectromech. Sys.*, vol. 18, no. 6, pp. 1401–08, 2009.
[25] M. Akgul *et al.*, "Capacitively Transduced Micromechanical Resonators with Simultaneous Low Motional Resistance and Q >70,000," Tech. Digest, *2008 Solid-State Sensor, Actuator, and Microsystems Wksp.*, Hilton Head, SC, June 6–10, 2010, pp. 467–70.
[26] Y.-W. Lin *et al.*, "Third-Order Intermodulation Distortion in Capacitively-Driven VHF Micromechanical Resonators," *Proc. IEEE Int'l. Ultrasonics Symp.*, Rotterdam, The Netherlands, Sept. 18-21, 2005, pp. 1592–95.
[27] Y. Lin *et al.*, "Enhancement of Micromechanical Resonator Manufacturing Precision via Mechanically-Coupled Arraying," *Proc. 2009 IEEE Int'l. Frequency Control Symp.*, Besancon, France, April 20-24, 2009, pp. 58–63.

[28] G. Maier, "The Search for Low-ε and Ultra-Low-ε Dielectrics: How Far Can You Get with Polymers? Part 1: Background," *IEEE Electrical Insulation Mag.*, Mar./Apr. 2004, pp. 6–17.
[29] W.-L. Huang, Z. Ren, and C. T.-C. Nguyen, "Nickel Vibrating Micromechanical Disk Resonator with Solid Dielectric Capacitive-Transducer Gap," *Proc. 2006 IEEE Int'l. Frequency Control Symp.*, Miami, FL, June 5–7, 2006, pp. 839–47.
[30] W.-L. Huang *et al.*, "Fully Monolithic CMOS Nickel Micromechanical Resonator Oscillator," *Tech. Digest, 21st IEEE Int'l. Conf. Micro Electro Mechanical Systems*, Tucson, AZ, Jan. 13–17, 2008, pp. 10–13.

BIOGRAPHY

CLARK T.-C. NGUYEN [S'90, M'95, SM'01, F'07] (ctnguyen@eecs.berkeley.edu) received his B. S., M. S., and Ph.D. degrees from the University of California at Berkeley in 1989, 1991, and 1994, respectively, all in electrical engineering and computer sciences. In 1995, he joined the faculty of the University of Michigan, Ann Arbor, where he was a professor in the Department of Electrical Engineering and Computer Science up until mid-2006. In 2006, he joined the Department of Electrical Engineering and Computer Sciences at the University of California at Berkeley, where he is presently a professor and co-director of the Berkeley Sensor & Actuator Center. His research interests focus on micro electromechanical systems (MEMS) and include integrated micromechanical signal processors and sensors, merged circuit/micromechanical technologies, RF communication architectures, and integrated circuit design and technology. In 2001, he founded Discera, Inc., the first company aimed at commercializing communication products based on MEMS technology, with an initial focus on the very vibrating micromechanical resonators pioneered by his research in past years. He served as vice president and chief technology officer (CTO) of Discera until mid-2002, at which point he joined DARPA on an IPA, where he served for three and a half years as the program manager for 10 different MEMS-centric programs in the Microsystems Technology Office of DARPA. He is presently serving as the Vice President for Frequency Control in the IEEE Ultrasonics Ferroelectrics and Frequency Control Society.